

# Prognostic role of three-dimensional speckle-tracking echocardiography-derived left ventricular global longitudinal strain in cardiac amyloidosis: Insights from the MAGYAR-Path Study

Dóra Földeák<sup>1</sup> | Árpád Kormányos<sup>2</sup> | Attila Nemes<sup>2</sup>

<sup>1</sup>Division of Haematology, Department of Medicine, Albert Szent-Györgyi Medical School, University of Szeged, Szeged, Hungary

<sup>2</sup>Department of Medicine, Albert Szent-Györgyi Medical School, University of Szeged, Szeged, Hungary

## Correspondence

Attila Nemes, Department of Medicine, Albert Szent-Györgyi Medical School, University of Szeged, Semmelweis Street 8, H-6725 Szeged, Hungary.

Email: [nemes.attila@med.u-szeged.hu](mailto:nemes.attila@med.u-szeged.hu)

## Abstract

**Introduction:** Systemic amyloidosis is an uncommon disorder in which amyloid fibrils deposit extracellularly. Three-dimensional speckle-tracking echocardiography (3DSTE) is a novel method able to assess left ventricular (LV) global longitudinal strain (GLS). Our aim was to evaluate the prognostic impact of 3DSTE-derived LV-GLS in patients with cardiac amyloidosis (CA).

**Materials and Methods:** A total of 35 patients suffering from light-chain (AL) CA or transthyretin (TTR) CA were selected, but 7 patients had to be excluded due to insufficient image quality or were lost for follow-up. With AL-CA 23 cases, while for TTR-CA 5 patients were diagnosed. Complete two-dimensional Doppler and 3DSTE were performed in all subjects.

**Results:** The median follow-up was 201 days (ranging from 36 to 632 days) during which cardiovascular event was detected in 17 CA patients, including 8 cardiac deaths. Six patients were diagnosed with acute heart failure, two patients needed invasive interventions (percutaneous coronary intervention with stent-implantation, implantable cardioverter defibrillator implantation) and in one patient new higher grade atrioventricular block was registered. Using ROC analysis, 3DSTE-derived LV-GLS  $\geq 11.8\%$  (absolute value) was found to be a significant predictor for cardiovascular event-free survival (sensitivity 65%, specificity 64%, area under the curve 0.71,  $p = .05$ ). Lower LV ejection fraction was confirmed in patients with LV-GLS  $< 11.8\%$  as compared to cases with LV-GLS  $\geq 11.8\%$ . In case of a cardiovascular event, LV-GLS was lower as compared to that of subjects with no events. Multivariable regression analysis confirmed that LV-GLS and LV end-diastolic diameter were independent predictors of cardiovascular survival.

**Conclusion:** 3DSTE-derived LV-GLS is an independent predictor for future cardiovascular events in CA patients.

## KEYWORDS

cardiac amyloidosis, global longitudinal strain, speckle-tracking, three-dimensional echocardiography

## 1 | INTRODUCTION

Systemic amyloidosis is an uncommon disorder in which protein (amyloid) fibrils composed of low-molecular weight subunits (5–25 kD) of various serum proteins deposit extracellularly.<sup>1</sup> The deposited amyloid fibrils damage the structure and function of the affected organs progressively causing diverse clinical symptoms.<sup>2,3</sup> A biopsy is required from the affected tissue or the abdominal fat pad for the diagnosis in most of the cases.<sup>4</sup> Amyloidosis is classified depending on the type of the precursor protein confirmed with immunochemistry by Congo-red positive tissue deposits or with mass spectrometry. Among the most common types acquired monoclonal immunoglobulin light-chain amyloidosis (AL), age-related wild-type (ATTRwt) and hereditary transthyretin amyloidosis (ATTRh) are listed. The mortality is especially elevated in AL amyloidosis.<sup>5,6</sup>

The AL amyloidosis is a systemic disease with some warning features like nephrotic syndrome, tissue infiltration (e.g., macroglossia), carpal tunnel syndrome, peripheral nervous system symptoms. This type of amyloidosis can often be present in multiple myeloma cases. In case of cardiac involvement, syncope is a common clinical sign, it presents quite frequently and is a poor prognostic factor.<sup>7</sup> Cardiac involvement in amyloidosis (CA) is most common in AL-CA and TTR-CA including both ATTRwt and ATTRh. The real incidence of CA is not known accurately, sadly it is often diagnosed only during autopsy.<sup>8</sup> Cardiac involvement is characterized by concentric ventricular thickening in the right ventricle (RV), normal or near normal left ventricular (LV) ejection fraction (EF) and valvular thickening.<sup>9,10</sup> The speckled or granular myocardial appearance is specific for amyloid deposit, but this phenomenon is often absent.<sup>2</sup> Diastolic dysfunction is one of the first signs of CA detected by echocardiography, it can often be detected before any clinical symptom develops.<sup>11,12</sup> The end-diastolic thickness of the interventricular septum (IVS) is  $>12$  mm and there is no other cause of LV hypertrophy is present in heart involvement.<sup>13</sup> In CA, the thickness of the LV wall does not correlate with the course and outcome of the disease.<sup>6</sup> Heart failure (HF) usually occurs in CA as a consequence of decreased myocardial compliance and compressed myocardial cells, because the infiltration by amyloid deposits lead to the development of restrictive cardiomyopathy.<sup>1</sup> Arrhythmias, pleural and pericardial effusion can also be detected in some cases.<sup>4,14,15</sup> The main goal regarding the treatment in both AL and TTR types is to eliminate or at least suppress the production of the amyloid proteins and improve the affected organ functions, including the heart, the kidney, the gastrointestinal tract and the peripheral nervous system.

Two-dimensional (2D) speckle-tracking echocardiography (STE)-derived LV global longitudinal strain (GLS) is known to have an independent, strong prognostic value even in AL amyloidosis.<sup>16</sup> Three-dimensional (3D) STE is a new, validated noninvasive imaging technique with capability to see the heart and its chambers including LV as a 3D organ. Moreover, it allows to measure volume-based functional properties and unidirectional and multidirectional strain parameters at the same time using the same 3D echocardiographic datasets.<sup>17</sup> Our aim was to evaluate the prognostic impact of 3DSTE-derived LV-GLS in CA patients.

## 2 | MATERIALS AND METHODS

### 2.1 | Patient population

A total of 35 patients with AL-CA or TTR-CA were selected from which 7 patients had to be excluded due to insufficient image quality or lost for follow-up. In the remaining group, with TTR-CA 5 patients, while for AL-CA 23 cases were diagnosed. TTR-CA proved to be ATTRh in 2 cases and ATTRwt in 3 cases. Patients were cared at the Division of Hematology, University of Szeged, Hungary, which serves as a tertiary center. Clinical and demographic features of CA patients are presented in Table 1. CA was defined in accordance with the current consensus criteria and practices.<sup>13,18</sup> Biopsy was performed from the bone marrow in 5 patients, from the subcutis in 4 patients, from the kidney in 9 patients, from the heart in 10 patients, from the gastrointestinal tract in 4 patients and from the salivary gland in 1 patient. In 5 cases, samples were collected from more than 1 organ. In patients with extracardiac biopsy positive for amyloid, the following echocardiographic criteria were used (unexplained LV wall thickness  $\geq 12$  mm  $+1$  or  $2$ )<sup>18</sup>:

1. Characteristic echocardiography findings ( $\geq 2$  of a, b and c have to be present):
  - a. Grade 2 or worse diastolic dysfunction.
  - b. Reduced tissue Doppler  $s'$ ,  $e'$ , and  $a'$  wave velocities ( $<5$  cm/s).
  - c. Decreased LV-GLS (absolute value  $< -15\%$ ).
2. Multiparametric echocardiographic score  $\geq 8$  points:
  - a. Relative LV wall thickness ( $(IVS + LV \text{ posterior wall [PW]}) / LV \text{ end-diastolic diameter} > 0.6$  (3 points).
  - b. Doppler E wave/ $e'$  wave velocities  $> 11$  (1 point).
  - c. Tricuspid annular plane systolic excursion  $\leq 19$  mm (2 points).
  - d. LV-GLS (absolute value)  $\leq -13\%$  (1 point).
  - e. Systolic longitudinal strain (LS) apex-to-base ratio  $> 2.9$  (3 points).

In the AL-CA group, lambda positivity was diagnosed in 14 cases, kappa positivity in 6 cases, in 8 cases it was not determined. In two cases from the AL-CA group, no information was available regarding their treatment. In all other AL-CA cases, different types of immunomodulatory treatment were administered. According to the international standard, in most cases, three drug-combination therapy was given with dexamethasone, proteasome inhibitor, immunomodulators or monoclonal antibody. In TTR-CA cases, tafamidis was administered in two cases. All patients with cardiac involvement were treated with the necessary HF medications. For cardiac evaluation, complete two-dimensional (2D) Doppler echocardiography and 3DSTE assessment were performed in all CA patients and controls. The present study was a part of the Motion Analysis of the heart and Great vessels by three-dimensional speckle-tracking echocardiography in Pathological cases (MAGYAR-Path) Study organized to evaluate changes in 3DSTE-derived parameters in various diseases compared to matched healthy volunteers as controls

TABLE 1 Clinical, echocardiographic and follow-up data of patients with cardiac amyloidosis

	All patients	LV-GLS $\geq -11.8\%$	LV-GLS $< -11.8\%$	LV-EF $\geq 55\%$	LV-EF $< 55\%$	No event	Event	AL-CA	TTR-CA
Clinical data									
No of patients	28	13 (46)	15 (54)	15 (54)	13 (46)	11 (39)	17 (61)	23 (82)	5 (18)
Males (%)	19 (68)	10 (77)	9 (60)	8 (53)	11 (85)	7 (64)	12 (71)	15 (65)	4 (80)
Age (years)	64.4 $\pm$ 8.7	63.5 $\pm$ 9.8	65.2 $\pm$ 7.4	62.3 $\pm$ 8.5	66.5 $\pm$ 8.4	64.5 $\pm$ 6.4	64.4 $\pm$ 9.9	63.6 $\pm$ 8.8	68.2 $\pm$ 6.7
Diabetes mellitus (%)	2 (7)	1 (8)	1 (7)	1 (7)	1 (8)	1 (9)	1 (6)	1 (4)	1 (20)
Hypertension (%)	16 (57)	7 (54)	9 (60)	9 (60)	7 (54)	7 (64)	9 (53)	14 (61)	2 (40)
Chronic renal failure (%)	6 (21)	4 (31)	2 (13)	4 (27)	2 (15)	2 (18)	4 (24)	6 (26)	0 (0)
Severe arrhythmia (%)	10 (36)	3 (23)	7 (47)	2 (13)	8 (62) <sup>†</sup>	1 (9)	9 (53) <sup>†</sup>	5 (22)	5 (100) <sup>#</sup>
TTR-CA (%)	5 (18)	1 (8)	4 (27)	0 (0)	5 (38) <sup>†</sup>	1 (9)	4 (24)	0 (0)	5 (100) <sup>#</sup>
Two-dimensional echocardiography									
LV-EDD (mm)	46.9 $\pm$ 4.0	47.3 $\pm$ 4.9	46.5 $\pm$ 2.9	47.5 $\pm$ 4.3	46.2 $\pm$ 3.6	49.6 $\pm$ 3.5	45.1 $\pm$ 3.2 <sup>†</sup>	47.2 $\pm$ 4.3	45.6 $\pm$ 1.6
LV-EDV (mL)	103.9 $\pm$ 24.9	112.3 $\pm$ 2.1	97.2 $\pm$ 18.2	103.5 $\pm$ 22.4	104.4 $\pm$ 27.3	117.3 $\pm$ 25.7	94.8 $\pm$ 19.6 <sup>†</sup>	107.7 $\pm$ 24.8	87.4 $\pm$ 17.2
LV-ESD (mm)	31.6 $\pm$ 4.9	30.2 $\pm$ 5.4	32.8 $\pm$ 4.1	29.3 $\pm$ 3.7	34.2 $\pm$ 4.9 <sup>†</sup>	32.4 $\pm$ 4.4	31.1 $\pm$ 5.1	31.1 $\pm$ 5.1	33.6 $\pm$ 3.7
LV-ESV (mL)	47.2 $\pm$ 18.0	26.2 $\pm$ 23.0	48.1 $\pm$ 12.5	37.0 $\pm$ 13.9	58.2 $\pm$ 15.3 <sup>†</sup>	50.6 $\pm$ 20.0	44.9 $\pm$ 1.60	46.0 $\pm$ 19.2	52.4 $\pm$ 9.5
IVS (mm)	15.9 $\pm$ 3.9	13.9 $\pm$ 1.8	17.7 $\pm$ 4.5*	13.5 $\pm$ 1.6	18.8 $\pm$ 3.9 <sup>†</sup>	14.2 $\pm$ 2.2	17.1 $\pm$ 4.4	14.4 $\pm$ 2.1	23.0 $\pm$ 2.6 <sup>#</sup>
LV-PW (mm)	14.6 $\pm$ 3.1	13.3 $\pm$ 1.9	15.7 $\pm$ 3.5*	13.0 $\pm$ 1.5	16.4 $\pm$ 3.4 <sup>†</sup>	13.5 $\pm$ 2.1	15.2 $\pm$ 3.4	13.6 $\pm$ 1.9	19.0 $\pm$ 3.6 <sup>#</sup>
LV-EF (%)	55.7 $\pm$ 13.9	62.8 $\pm$ 10.3	49.6 $\pm$ 13.7*	66.3 $\pm$ 6.6	43.6 $\pm$ 9.6 <sup>†</sup>	61.7 $\pm$ 9.4	51.9 $\pm$ 14.9	59.3 $\pm$ 11.3	39.4 $\pm$ 13.1 <sup>#</sup>
Three-dimensional speckle-tracking echocardiography									
LV-EDV (mL)	79.1 $\pm$ 23.7	82.0 $\pm$ 22.9	76.0 $\pm$ 24.3	71.9 $\pm$ 14.1	92.7 $\pm$ 31.1 <sup>†</sup>	79.8 $\pm$ 19.0	78.6 $\pm$ 26.8	79.1 $\pm$ 23.7	106.8 $\pm$ 46.3
LV-ESV (mL)	42.0 $\pm$ 19.9	35.9 $\pm$ 18.3	48.7 $\pm$ 19.5	32.6 $\pm$ 10.5	59.9 $\pm$ 21.1 <sup>†</sup>	38.0 $\pm$ 12.2	45.1 $\pm$ 23.8	42.0 $\pm$ 19.9	73.9 $\pm$ 37.8 <sup>#</sup>
LV-EF (%)	47.9 $\pm$ 14.6	57.8 $\pm$ 10.2	37.0 $\pm$ 10.4*	54.6 $\pm$ 11.8	35.3 $\pm$ 10.5 <sup>†</sup>	52.5 $\pm$ 10.0	44.3 $\pm$ 16.5	47.9 $\pm$ 14.6	32.1 $\pm$ 7.9 <sup>#</sup>
LV-mass (g)	143.3 $\pm$ 34.0	137.2 $\pm$ 24.2	150.0 $\pm$ 41.1	134.8 $\pm$ 27.1	159.3 $\pm$ 39.4	141.5 $\pm$ 29.1	144.7 $\pm$ 37.2	143.3 $\pm$ 34.0	169.1 $\pm$ 105.2
LV-GLS (%)	11.7 $\pm$ 5.2	16.2 $\pm$ 3.4	7.7 $\pm$ 2.7*	-14.6 $\pm$ 4.7	-8.3 $\pm$ 3.5 <sup>†</sup>	14.2 $\pm$ 4.9	10.1 $\pm$ 4.8 <sup>†</sup>	12.4 $\pm$ 5.3	8.4 $\pm$ 3.0
Pts with LV-GLS $< -11.8\%$	15 (54)	0 (0)	15 (100)*	5 (33)	10 (77) <sup>†</sup>	4 (36)	11 (65)	11 (48)	4 (80)
Events									
Pts with events (%)	17 (61)	6 (46)	11 (73)	7 (47)	10 (77)	0 (0)	17 (100) <sup>†</sup>	13 (57)	4 (80)
Pts with death (%)	8 (29)	4 (31)	4 (27)	4 (27)	4 (31)	2 (18)	8 (47)	8 (35)	0 (0)

Abbreviations: AL-CA, light-chain cardiac amyloidosis; EDD, end-diastolic diameter; EDV, end-diastolic volume; EF, ejection fraction; ESD, end-systolic diameter; ESV, end-systolic volume; GLS, global longitudinal strain; IVS, interventricular septum; LV, left ventricular; PW, posterior wall; TTR-CA, transthyretin cardiac amyloidosis.

\* $p < .05$  versus patients with LV-GLS  $\geq -11.8\%$ .

<sup>†</sup> $p < .05$  versus patients with no event.

<sup>#</sup> $p < .05$  versus patients with AL-CA.

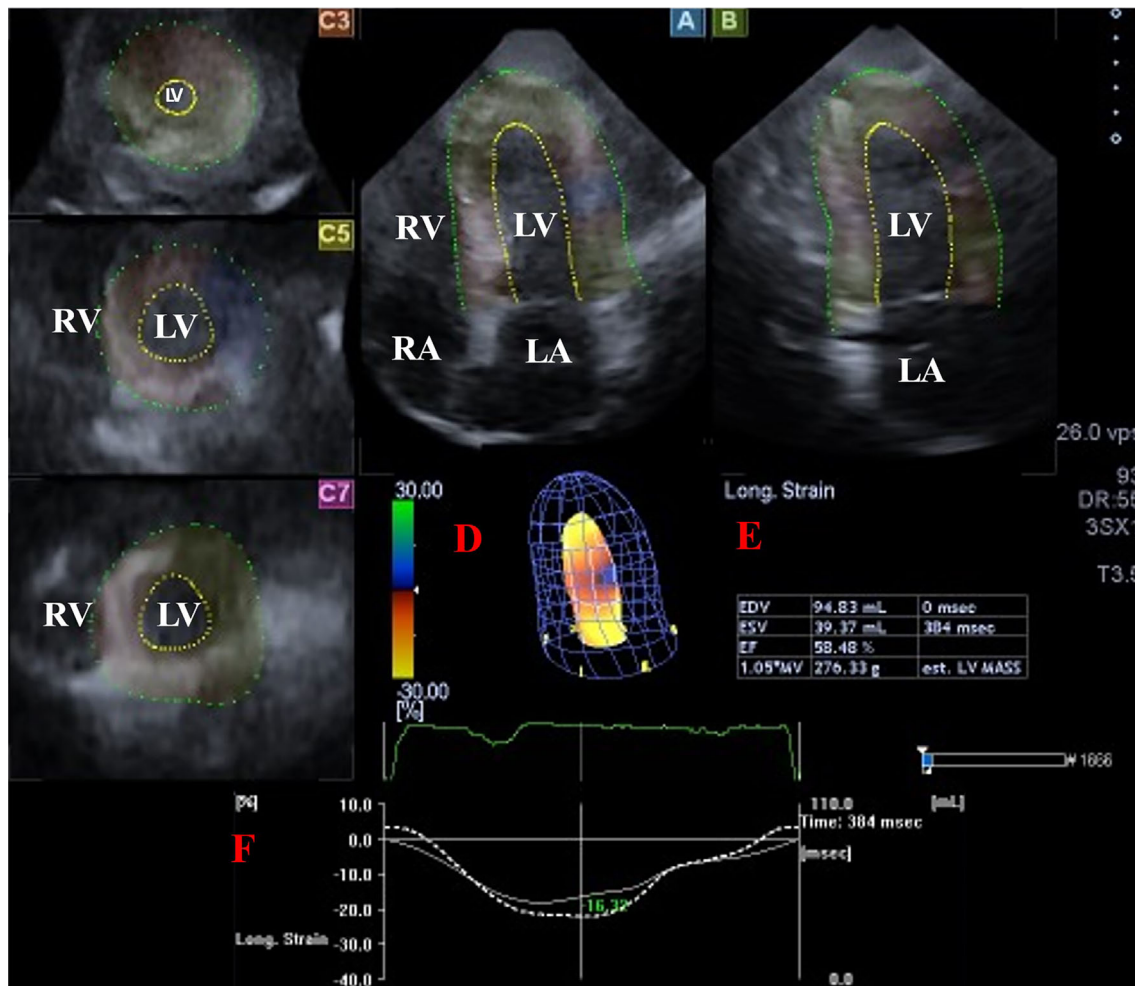


**FIGURE 1** Analysis of the left ventricle (LV) from a three-dimensional (3D) speckle-tracking echocardiographic dataset: (A) apical four-chamber view, (B) apical two-chamber view and (C3) apical, (C5) mid-ventricular, and (C7) basal LV short-axis views. A virtual 3D cast of the LV (red D), LV volumetric data respecting the cardiac cycle (red E), LV global longitudinal strain curve (GLS, white line) and time-LV volume changes (dashed line) during the cardiac cycle (red F) are presented in a patient with cardiac amyloidosis. LV, left ventricle; LA, left atrium; RV, right ventricle; RA, right atrium

(“magyar” means “Hungarian” in Hungarian language). The study protocol was prepared in accordance with the ethical guidelines of the 1975 Declaration of Helsinki (and updated versions) and was approved by the Institutional and Regional Human Biomedical Research Committee of University of Szeged (Hungary) (protocol number: 71/2011). Informed consent was obtained from each study participant.

## 2.2 | Two-dimensional Doppler echocardiography

During 2D echocardiography, gray-scale harmonic images were acquired in the lateral decubitus position, using a commercially available ultrasound system (Artida™, Toshiba Medical Systems, Tokyo, Japan) with a broadband 1–5 MHz PST-30BT phased-array transducer. Chamber dimensions, volumes and LV-EF were measured using 2D Doppler echocardiography in accordance with the

recommendations.<sup>19,20</sup> 2DSTE-derived LV analyses were performed on loops recorded on apical four- (AP4CH) and two-chamber (AP2CH) views. The severity of mitral and tricuspid regurgitations was determined with visual assessment using color Doppler echocardiography.

## 2.3 | Three-dimensional speckle-tracking echocardiography

3D echocardiographic datasets were acquired with the same Toshiba Artida™ ultrasound system using a 1–4 MHz PST-25SX matrix phased-array transducer.<sup>17</sup> After optimizing the gain setting, wide-angled images were recorded. Six wedge-shaped subvolumes focused on LV were acquired over six consecutive cardiac cycles during a single breath-hold and constant RR interval. The mean frame rate proved to be  $30 \pm 2$  fps. A full volume pyramidal 3D dataset was created

automatically, LV chamber quantification was performed offline using 3D Wall Motion Tracking software version 2.7 (Toshiba Medical Systems, Tokyo, Japan). Each 3D dataset was displayed in a 5-plane view: an AP4CH view, an AP2CH view and three short-axis views. A virtual 3D model of the LV was created following manual definition of the LV endocardium at the edges of the mitral valve and the LV apex on AP2CH and AP4CH views. Automatic reconstruction was performed and the endocardium was tracked throughout the cardiac cycle. After, LV-GLS, the most frequently used parameter featuring LV contractility and function was then calculated (Figure 1). Apical-to-basal LV segmental LS ratio was defined as LV segmental LSs of apical segments divided by LV segmental LSs of basal segments. The apical sparing ratio was also calculated as a ratio of average apical LV-LS divided by (average basal LV-LS + average midventricular LV-LS). The peak value of LV-GLS was defined as its maximum absolute value with a positive sign.

## 2.4 | Statistical analysis

All continuous variables were presented as mean  $\pm$  standard deviation. Categorical data were indicated as frequencies and percentages (%). Kolmogorov–Smirnov test was used to test data for normality. Student's *t*-test was used in case of normal distribution, while Mann–Whitney–Wilcoxon test was applied for non-normally distributed datasets. For analysis of categorical variables, Fisher's exact test was adopted. Survival of patients was evaluated with Kaplan–Meier life table estimates during the follow-up. Long-rank test was used to determine potential differences in survival rates between groups. The predictive power of LV-GLS was determined with receiver operator curves (ROCs), sensitivity and specificity values were calculated from the area under the curve. All tests were two-sided and a *p*-value below .05 was considered statistically significant. Echocardiographic variables associated with the study primary outcome were investigated by univariate analysis. In case of values found to be significant with univariable analysis (*p* < .10), Cox proportional hazard modeling was used as a multivariate approach with a forward stepwise model to analyze independent predictors of survival. Parametric statistical analysis was used to compare the patient groups. SPSS software (SPSS Inc., Chicago, IL, USA) was used for the statistical analysis.

## 3 | RESULTS

### 3.1 | Clinical and demographic data

Clinical and demographic data are presented in Table 1. Patients with events had more severe arrhythmia episodes (atrial fibrillation or flutter, ventricular tachycardia, higher grade atrioventricular block) in their medical history than patients without events. TTR-CA patients had more severe arrhythmia in their medical history than AL-CA patients.

### 3.2 | Two-dimensional echocardiography

Routine 2D echocardiographic data are presented in Table 1. IVS and LV-(PW) were thicker and LV-EF was decreased in patients with 3DSTE-derived LV-GLS <−11.8% compared to cases with LV-GLS  $\geq$ −11.8%. Patients with events had smaller LV end-diastolic dimensions as compared to that of subjects with no events. Patients with TTR-CA had thicker IVS and LV-PW and lower LV-EF as compared to that of AL-CA.

### 3.3 | Three-dimensional speckle-tracking echocardiography

3DSTE data are presented in Table 1. Apical-to-basal segmental LV-LS ratio proved to be  $3.2 \pm 3.1$ . The apical sparing ratio was  $0.98 \pm 0.07$ . Lower LV-EF could be detected in patients with LV-GLS <11.8% as compared to cases with LV-GLS  $\geq$ 11.8%. Patients with events had lower LV-GLS as compared to that of subjects with no events. Patients with TTR-CA had thicker IVS and LV-PW and lower LV-EF as compared to that of AL-CA.

### 3.4 | Global longitudinal strain

3DSTE-derived LV-GLS were lower than those obtained by 2DSTE ( $11.7\% \pm 5.2\%$  vs.  $14.0\% \pm 4.5\%$ , *p* < .05). Using ROC analysis, 3DSTE-derived LV-GLS  $\geq$ 11.8% was a significant predictor for cardiovascular event-free survival (sensitivity 65%, specificity 64%, area

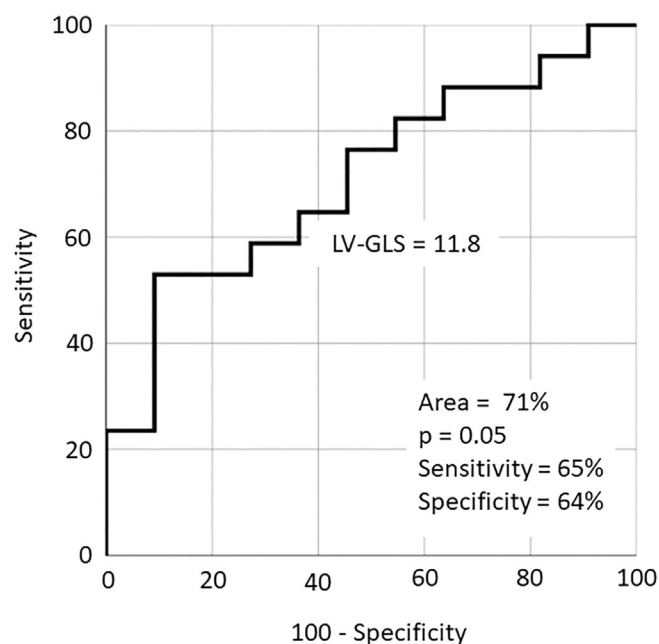


**FIGURE 2** Receiver operating characteristic analysis illustrating the diagnostic accuracy of three-dimensional speckle-tracking echocardiography-derived global longitudinal strain (GLS) in predicting cardiovascular morbidity and mortality

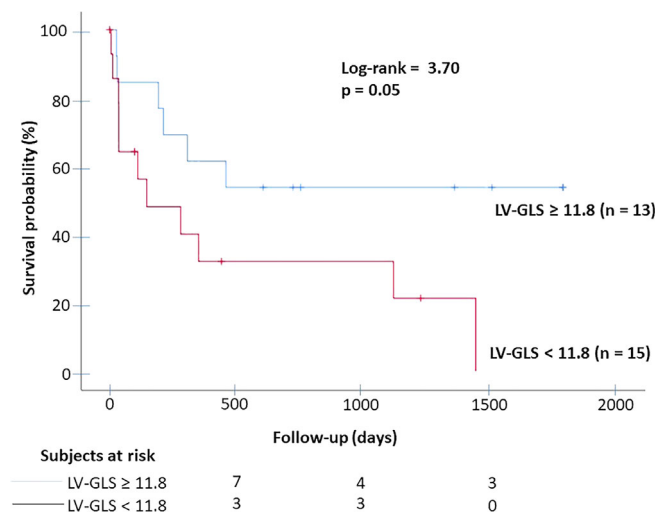


**FIGURE 3** Kaplan–Meier survival curves illustrating the predictive role of three-dimensional speckle-tracking echocardiography-derived left ventricular global longitudinal strain (GLS)

under the curve 0.71,  $p = .05$ ; Figure 2). The Kaplan–Meier cumulative survival curve illustrating the predictive role of 3DSTE-derived LV-GLS is presented in Figure 3.

### 3.5 | Ejection fraction

CA patients with reduced LV-EF had more arrhythmia, lower LV-GLS, higher LV end-systolic diameter and volume and more increased LV thickness. All patients with reduced LV-EF proved to have TTR-CA and patients with normal LV-EF had only AL-CA. Survival was not significantly different between CA subjects with reduced vs. normal LV-EF (Table 1).

### 3.6 | Events

During a median follow-up of 201 days (interquartile range 36–632 days), 17 CA patients suffered cardiovascular event including 8 cardiac deaths. Acute HF developed in six patients, two patients underwent invasive interventions (percutaneous coronary intervention with stent-implantation, implantable cardioverter defibrillator implantation) and one patient had new higher grade atrioventricular block. During the follow-up, survival was better in the TTR-CA subjects than among subjects with AL-CA (Table 1).

### 3.7 | Multivariable analysis

By univariable analysis, reduced LV end-diastolic diameter, thicker IVS and lower LV-GLS were significant predictors of cardiovascular events. Multivariable regression analysis showed that LV-GLS (hazard ratio [HR] = 3.2, 95% CI of HR: 1.65–5.1,  $p < .05$ ) and LV end-diastolic diameter (HR = 2.8, 95% CI of HR: 1.61–4.32,  $p < .05$ ) were independent predictors of cardiovascular survival.

## 4 | DISCUSSION

Amyloid protein deposition causes organ failure, cardiac involvement with myocardial invasion is a severe complication in AL and ATTR amyloidosis. High chance for arrhythmias and HF contribute to a poorer quality of life in amyloidosis. In those cases when the heart is not involved, the survival is 4 years,<sup>21</sup> in some severe CA cases, it is only 8 months.<sup>22</sup>

Due to recent advances in cardiovascular imaging, novel echocardiographic techniques came into practice including STE and/or 3D echocardiography. 3DSTE combines advantages of both methods: volumetric and strain analysis could be performed at the same time using the same virtual model of the LV respecting cardiac cycle. It could be expected that 3DSTE-derived variables including strains (for instance LV-GLS) has a strong prognostic impact in certain disorders as in CA.

Previously, only 2DSTE was a method of choice for the clinical assessment of LV strains with significant technical and theoretic limitations. Nevertheless, 2DSTE-derived LV-GLS was found to be a strong predictor of survival in patients with AL amyloidosis undergoing hematopoietic stem cell transplantation, potentially providing incremental value over serum cardiac biomarkers for risk stratification.<sup>23</sup> In a recent study with the novel 3DSTE, LV-GLS  $\leq 14.8\%$  and cardiac troponin T  $\geq 0.049$  mg/L levels were independent predictors of survival in CA.<sup>24</sup> In another study, patients with LV-GLS  $< 14.2\%$  had a corresponding median overall survival and 5-year overall survival rate of 33.2 months and 39%, respectively, versus 7.7 months and 6% for those with LV-GLS  $\geq 14.2\%$ . This difference was maintained despite further stratification by revised Mayo stage.<sup>25</sup> The more recent and advanced magnetic resonance imaging (MRI) feature tracking strain was also found to be associated with all-cause mortality in patients with AL amyloidosis.<sup>26</sup> The incremental prognostic value of cardiac MRI-derived LV-GLS was found in AL amyloidosis refining conventional risk evaluation based on LV late gadolinium enhancement (LGE).<sup>27</sup> Reduced relative apical LS assessed by echocardiography significantly correlated with reduced survival in patients with late-onset hereditary TTR amyloidosis with p.A97S variant.<sup>28</sup> In contrast, echocardiography-based assessment of LV-GLS did not predict all-cause mortality in another study.<sup>29</sup> However, by combining LV myocardial work index and apical-to-basal segmental work ratio, an independent model for all-cause mortality prediction was obtained.<sup>29</sup> Over LV dysfunction, RV dysfunction appears also to be an independent determinant of outcome in patients with amyloidosis.<sup>27,30,31</sup> Although prognostic value of MRI-derived RV-LGE was also confirmed,<sup>27</sup> RV free wall LS was found to be a better predictor of all-cause mortality than RV-EF, RV fractional area change, or RV-GLS.<sup>30</sup> Our findings confirmed these findings demonstrating prognostic impact of 3DSTE-derived LV-GLS in CA. Moreover, survival did not differ between CA patients with reduced versus normal LV-EF. Although all TTR-CA patients had reduced LV-EF, their survival proved to be better as compared to that of AL-CA cases.

With the evaluation of the 3DSTE-derived LV-GLS, the detection of the cardiac involvement can be confirmed early and the sooner we start the treatment, the better outcome the patient can expect. Moreover, 3DSTE-derived volumetric data including LV-EF is more accurate and closer to the reality than that of one derived by 2D echocardiography.

## 4.1 | Limitation section

- It should be considered that CA is a rare disease, all but only a limited number of CA patients with confirmed diagnosis was involved into the MAGYAR-Path Study between 2011 and 2021. However, from 120 patients with heart failure with preserved LV-EF, 16 showed wild-type transthyretin amyloidosis (13%) in a recent prospective study. This finding might be explained with significant number of underdiagnosed cases.<sup>32</sup>
- The number of CA patients is really small in this study mixing results of AL-CA and TTR-CA patients. However, the follow-up and prognosis are not the same for them, therefore results should be considered and interpreted according to these facts.
- The aim of this study was only to evaluate the prognostic impact of 3DSTE-derived LV-GLS. Assessment of other LV parameters or deformation variables of other heart chambers were not aimed to be evaluated.
- The image quality of 3DSTE-derived images is worse than that of images assessed by 2D echocardiography.
- Due to technical reasons, only patients with sinus rhythm could be examined by 3DSTE.
- The follow-up time was short and the TTR amyloidosis cohort was very advanced, which made it difficult to assess the clinical follow-up.
- TTR amyloidosis can be diagnosed without biopsy if monoclonal gammopathy is ruled out.<sup>18,33</sup>
- In the present study, ATTRh and ATTRwt were also appeared. However, depending on the genetic mutation, echocardiographic parameters and predictors differ between ATTRwt and ATTRh, which could affect results.<sup>34</sup>
- The wall thickness was higher in those with a GLS <11.8%, which seems to be driven by the ATTR cohort. It was not the same for just the AL cohort. Based on results, thicker wall thickness seems to have effects on prediction of survival, which could be considered, when interpreting findings.
- The study would have been stronger if different cardiac stages were examined as done in a recent paper.<sup>33</sup> Moreover, impairment of baseline GLS and an absolute improvement in GLS were found to be profitable additional measures considering the prognosis and the response to therapy in AL-CA.

## 5 | CONCLUSION

3DSTE-derived LV-GLS is an independent predictor of a cardiovascular event in CA patients.

### AUTHOR CONTRIBUTIONS

**Dóra Földeák:** Investigation, Data curation, Resources, Writing—original draft. **Árpád Kormányos:** Methodology, Software, Investigation, Data curation, Writing—review and editing. **Attila Nemes:** Conceptualization, Writing—original draft, Writing—review and editing.

### CONFLICT OF INTEREST STATEMENT

The authors declare no conflict of interest.

### DATA AVAILABILITY STATEMENT

The data that support the findings of this study are available on request from the corresponding author. The data are not publicly available due to privacy or ethical restrictions.

### REFERENCES

1. Dubrey SW, Hawkins PN, Falk RH. Amyloid diseases of the heart: assessment, diagnosis, and referral. *Heart*. 2011;97:75-84.
2. Banyersad SM, Moon JC, Whelan C, Hawkins PN, Wechalekar AD. Updates in cardiac amyloidosis: a review. *J Am Heart Assoc*. 2012;1:e000364.
3. Westermark P, Benson MD, Buxbaum JN. A primer of amyloid nomenclature. *Amyloid*. 2007;14:179-183.
4. Falk RH. Diagnosis and management of the cardiac amyloidoses. *Circulation*. 2005;112:2047-2060.
5. Westermark P, Benson MD, Buxbaum JN, et al. Amyloid protein fibril nomenclature. *Amyloid*. 2002;9:197-200.
6. Rapezzi C, Merlini G, Quarta CC, et al. Systemic cardiac amyloidoses disease profiles and clinical courses of the 3 main types. *Circulation*. 2009;120:1203-1212.
7. Chamarthi B, Dubrey SW, Cha K, Skinner M, Falk RH. Features and prognosis of exertional syncope in light-chain associated AL cardiac amyloidosis. *Am J Cardiol*. 1997;80:242-245.
8. Gutierrez PS, Fernandes F, Mady C, Higuchi ML. Clinical, electrocardiographic and echocardiographic findings in significant cardiac amyloidosis detected only at necropsy: comparison with cases diagnosed in life. *Arq Bras Cardiol*. 2008;90:191-196.
9. Patel AR, Dubrey SW, Mendes LA, et al. Right ventricular dilation in primary amyloidosis: an independent predictor of survival. *Am J Cardiol*. 1997;80:486-492.
10. Porciani MC, Lilli A, Peretto F, et al. Tissue Doppler and strain imaging: a new tool for early detection of cardiac amyloidosis. *Amyloid*. 2009;16:63-70.
11. Tsang W, Lang RM. Echocardiographic evaluation of cardiac amyloid. *Curr Cardiol Rep*. 2010;12:272-276.
12. Bellavia D, Pellikka PA, Abraham TP, et al. Evidence of impaired left ventricular systolic function by Doppler myocardial imaging in patients with systemic amyloidosis and no evidence of cardiac involvement by standard two-dimensional and Doppler echocardiography. *Am J Cardiol*. 2008;101:1039-1045.
13. Gertz MA, Comenzo R, Falk RH, et al. Definition of organ involvement and treatment response in immunoglobulin light chain amyloidosis (AL): a consensus opinion from the 10th international symposium on amyloid and amyloidosis, Tours, France, 18-22 April 2004. *Am J Hematol*. 2005;79:319-328.
14. Brodarick S, Paine R, Higa E, Carmichael KA. Pericardial tamponade, a new complication of amyloid heart disease. *Am J Med*. 1982;73:133-135.
15. Navarro JF, Rivera M, Ortuno J. Cardiac tamponade as presentation of systemic amyloidosis. *Int J Cardiol*. 1992;36:107-108.
16. Barros-Gomes S, Williams B, Nhola LF, et al. Prognosis of light chain amyloidosis with preserved LVEF: added value of 2D speckle-tracking echocardiography to the current prognostic staging system. *JACC Cardiovasc Imaging*. 2017;10:398-407.
17. Nemes A, Kalapos A, Domsik P, Forster T. Three-dimensional speckle-tracking echocardiography—a further step in non-invasive three-dimensional cardiac imaging. *Orv Hetil*. 2012;153:1570-1577.
18. Garcia-Pavia P, Rapezzi C, Adler Y, et al. Diagnosis and treatment of cardiac amyloidosis: a position statement of the ESC Working Group of Myocardial and Pericardial Diseases. *Eur Heart J*. 2021;42:1554-1568.

19. Lang RM, Bierig M, Devereux RB, et al. American Society of Echocardiography's Nomenclature and Standards Committee; Task Force on Chamber Quantification; American College of Cardiology Echocardiography Committee; American Heart Association; European Association of Echocardiography, European Society of Cardiology. Recommendations for chamber quantification. *Eur J Echocardiogr.* 2006;7:79-108.
20. Rudski LG, Lai WW, Afilalo J, et al. Guidelines for the echocardiographic assessment of the right heart in adults: a report from the American Society of Echocardiography. *J Am Soc Echocardiogr.* 2010; 23:685-713.
21. Merlini G, Stone MJ. Dangerous small B-cell clones. *Blood.* 2006;108: 2520-2530.
22. Dispenzieri A, Gertz MA, Kyle RA, et al. Serum cardiac troponins and N-terminal pro-brain natriuretic peptide: a staging system for primary systemic amyloidosis. *J Clin Oncol.* 2004;22:3751-3757.
23. Shawn CP, Heather JL, Elyn RR, et al. Prognostic and added value of two-dimensional global longitudinal strain for prediction of survival in patients with light chain amyloidosis undergoing autologous hematopoietic cell transplantation. *J Am Soc Echocardiogr.* 2018;31:64-70.
24. Changhui L, Xiaoli Z, David HH, et al. Predictors of cardiac involvement and survival in patients with primary systemic light-chain amyloidosis: roles of the clinical, chemical, and 3-D speckle tracking echocardiography parameters. *BMC Cardiovasc Disord.* 2021;21:43.
25. Lee CK, Drill E, Yang JC, et al. Incremental value of global longitudinal strain for predicting survival in patients with advanced AL amyloidosis. *JACC CardioOncol.* 2020;2:223-231.
26. Jeffery EI, Shivaram PA, Arvin A, et al. MRI feature tracking strain is prognostic for all-cause mortality in AL amyloidosis. *Amyloid.* 2018; 25:101-108.
27. Xiao L, Jian L, Lu L, et al. Left and right ventricular myocardial deformation and late gadolinium enhancement: incremental prognostic value in amyloid light-chain amyloidosis. *Cardiovasc Diagn Ther.* 2020; 10:470-480.
28. Hsing-Jung L, Kuan-Chih H, Yun-Chieh L, et al. Cardiac manifestations and prognostic implications of hereditary transthyretin amyloidosis associated with transthyretin Ala97Ser. *J Formos Med Assoc.* 2020;119:693-700.
29. Tor SC, Hans E, Bertil L, et al. Prognostic implications of left ventricular myocardial work indices in cardiac amyloidosis. *Eur Heart J Cardiovasc Imaging.* 2021;22:695-704.
30. Wan K, Lin J, Guo X, et al. Prognostic value of right ventricular dysfunction in patients with AL amyloidosis: comparison of different techniques by cardiac magnetic resonance. *J Magn Reson Imaging.* 2020;52:1441-1448.
31. Liu H, Fu H, Guo YK, et al. The prognostic value of right ventricular deformation derived from cardiac magnetic resonance tissue tracking for all-cause mortality in light-chain amyloidosis patients. *Cardiovasc Diagn Ther.* 2020;10:161-172.
32. González-López E, Gallego-Delgado M, Guzzo-Merello G, et al. Wild-type transthyretin amyloidosis as a cause of heart failure with preserved ejection fraction. *Eur Heart J.* 2015;36:2585-2594.
33. Cohen OC, Ismael A, Pawarova B, et al. Longitudinal strain as an independent predictor of survival and response to therapy in patients with systemic AL amyloidosis. *Eur Heart J.* 2022;43:333-341.
34. Chacko L, Martone R, Bandera F, et al. Echocardiographic phenotype and prognosis in transthyretin cardiac amyloidosis. *Eur Heart J.* 2020; 41(14):1439-1447.

**How to cite this article:** Földeák D, Kormányos Á, Nemes A. Prognostic role of three-dimensional speckle-tracking echocardiography-derived left ventricular global longitudinal strain in cardiac amyloidosis: Insights from the MAGYAR-Path Study. *J Clin Ultrasound.* 2023;51(6):952-959. doi:[10.1002/jcu.23445](https://doi.org/10.1002/jcu.23445)